The F-box-like protein FBL17 is a regulator of DNA-damage response and co-localizes with RETINOBLASTOMA RELATED 1 at DNA lesion sites

Naomie Gentric, Kinda Masoud, Robin P. Journot, Valerie Cognat, Marie-Edith Chaboute, Sandra Noir, Pascal Genschik

The Arabidopsis F-box FBL17 co-localizes with γH2AX and its mutation leads to a constitutive DNA damage response.

The Arabidopsis F-box protein FBL17 is a constitutive (negative?) regulator of DNA damage response and co-localizes with γH2AX foci (upon genotoxic stress?)

Naomie Gentric[1], Kinda Masoud[1], Robin Journot[1], Valérie Cognat[1], Marie-Edith Chabouté[1], Sandra Noir[1*] and Pascal Genschik[1*]

1 Institut de Biologie Moléculaire des Plantes, Centre National de la Recherche Scientifique, Unité Propre de Recherche 2357, Conventionnée avec l'Université de Strasbourg, 67084 Strasbourg, France.

* Correspondence to:
Pascal Genschik, Institut de Biologie Moléculaire des Plantes (CNRS), 12, rue du Général Zimmer 67084 Strasbourg, France. Tel.: +33 3 88 41 72 78; E-mail: pascal.genschik@ibmp-cnrs.unistra.fr
Sandra Noir, Institut de Biologie Moléculaire des Plantes (CNRS), 12, rue du Général Zimmer 67084 Strasbourg, France. Tel.: +33 3 88 41 53 38; E-mail: sandra.noir@ibmp-cnrs.unistra.fr

ABSTRACT

In Arabidopsis, the F-box protein FBL17 (F BOX-LIKE17) was previously identified as an important cell cycle regulatory protein required for cell division during pollen development and for normal cell cycle progression and endoreplication during the diploid sporophyte phase. FBL17 was reported to control the stability of the CDK (CYCLIN-DEPENDENT KINASE) inhibitor KIP-RELATED PROTEINs (KRPs) which could explain the drastic reduction of cell division activity in both shoot and root apical meristems observed in *fbl17* loss-of-function mutants. However, whether this F-box protein has other substrates and functions besides degrading KRPs is currently unknown. Here we show that the mutation of *FBL17* leads not only to misregulation of cell cycle genes, but also to a strong upregulation of genes involved in DNA damage and repair processes. This phenotype is associated with a higher frequency of DNA lesions in *fbl17* and increased cell death in the root meristem even in absence of genotoxic stress. Notably, the constitutive activation of DNA damage response (DDR) genes is largely SOG1-independent in *fbl17*. In addition, we found that *fbl17* mutants are hypersensitive to DNA double-strand break (DSB)-induced genotoxic stress, which was monitored by root elongation, accumulation of cell death and occurrence of γH2AX foci. Interestingly, we observed that the FBL17 protein is recruited at nuclear foci upon DSB induction and co-localizes with γH2AX, but only in presence of RBR1. Altogether, our results highlight a novel function of FBL17 in DDR, likely by ubiquitylating proteins involved in DNA damage-signaling or repair.

INTRODUCTION

In all eukaryotes, the cell cycle is composed of four phases: in S phase DNA replication occurs and in mitosis (M) phase, chromosomes segregate into two nuclei, followed by cytokinesis, allowing cells to be divided into two daughter cells (Nurse, 2000). These two phases are separated by two gap phases (G1 and G2) during which cells increase their size, number of organelles and are subjected to cell cycle checkpoints. The proper orchestration of the cell cycle requires numerous levels of control. In particular, cyclin-dependent kinases (CDKs), activated by cyclins, are crucial players in this process and their activities are strictly regulated (Malumbres and Barbacid, 2005)(De Veylder et al., 2007). For instance, several CDKs are inactivated by cyclin-dependent kinase inhibitors CKIs (Denicourt and Dowdy, 2004) and both in fungi and metazoans, it has been established that CKI degradation at the G1-to-S transition releases CDK activity, which in turn is required to enter S phase. In budding yeast, this is achieved by the ubiquitin E3 ligase complex SCF^{Cdc4} (Skp1, Cdc53/CULLIN, and Cdc4, a WD40-type F-box protein), which ubiquitylates the CKI Sic1 protein leading to its proteolysis shortly before S phase (Schwob et al., 1994)(Feldman et al., 1997). Similarly, in mammalian cells, the CKI protein p27Kip1 becomes unstable when cells enter S phase, as targeted by the SCF^{SKP2} (SKP2 being a leucine rich repeat-containing F-box protein) ubiquitin ligase (reviewed in (Starostina and Kipreos, 2012). Notably, the human SCF^{SKP2} E3 targets also several other essential regulators of S-phase progression as well as other regulatory proteins.

Whether a similar regulation also occurs in plants is still not fully understood, but the Arabidopsis F-box protein FBL17 has been proposed to mediate such a process. *FBL17* loss-of-function mutants fail to undergo pollen mitosis II, which normally generates the two sperm cells in a mature pollen grain (Kim et al., 2008)(Gusti et al., 2009). This major cell cycle defect could be, at least partially, suppressed by the mutation of some *CKI* genes, called *KIP-RELATED PROTEINs* (*KRP*s) (Gusti et al., 2009)(Zhao et al., 2012). As some viable, though sterile, *fbl17* loss-of-function plants could be recovered, it was possible to show that these mutants accumulate a higher level of the KRP2 CKI protein and share some phenotypic characteristics with plants overexpressing KRP proteins (Noir et al., 2015). However, it also appeared that *fbl17* mutant plants exhibited some characteristics not observed in KRP overexpressors, suggesting that this F-box protein might have other targets and functions. In particular we observed in *fbl17* mutant root tips the occurrence of cell death and abnormal chromosome segregations, suggesting defects in genome stability (Noir et al., 2015).

The maintenance of genome integrity requires efficient DNA damage sensing and repair mechanisms (Cools and De Veylder, 2009)(Nisa et al., 2019). Cells are constantly subjected to DNA damages that arise from multiple origins such as replication errors, mutations induced by the production of reactive oxygen species or exposure to UV light, among others. However most of them, will be detected and efficiently repaired by several DNA repair pathways (reviewed in (Spampinato, 2017)). For cells, the most deleterious type of DNA damage are double strand breaks (DSBs), which can lead to chromosomal rearrangements, loss of genetic information and eventually to cell death (Amiard et al., 2013). DSBs induce a DNA damage response (DDR) which activates both cycle checkpoints and DNA repair pathways (Hu et al., 2016). At the molecular level, when DSB occurs on chromatids, these DSB are recognized by the MRE11-RAD50-NBS1 (MRN) complex (Syed and Tainer, 2018), which recruits ataxia telangiectasia mutated (ATM) kinase. Note that another kinase, ATM- and RAD3-related (ATR), is not activated by DSBs but rather by single-stranded DNA damage and replication fork stalling. Upon ATM activation, the kinase phosphorylates a multitude of downstream proteins involved in DDR. Among them, ATM phosphorylates the plant-specific transcription factor SUPPRESSOR OF GAMMA RESPONSE 1 (SOG1) (Yoshiyama et al., 2013), which plays a central role in DDR, by activating the expression of genes that participate in DNA repair, cell cycle arrest and cell death (Yoshiyama et al., 2009)(Bourbousse et al., 2018). For instance, SOG1 binds to the promoters and induces the expression of B1-type cyclin CYCB1;1 (Weimer et al., 2016), CDK inhibitors SIAMESE-RELATED 5 (SMR5) and SMR7 (Yi et al., 2014) and the DNA repair protein BRCA1 (Sjogren et al., 2015). Another important target of ATM is the histone variant H2AX, which upon phosphorylation becomes γ-H2AX (Friesner et al., 2005). Gamma-H2AX form foci at DSB sites which are important for the recruitments of DNA repair proteins such as RAD51 and BRCA1 (Biedermann et al., 2017; Horwarth et al., 2017). Strikingly, cell cycle regulators are not only transcriptionally regulated during DDR, but may also directly participate in the repair mechanism. Indeed, it has recently been reported that upon DNA damage, the Arabidopsis RETINOBLASTOMA RELATED (RBR1) protein and its binding partner E2FA are recruited to close to heterochromatic γH2AX-labelled foci in an ATM- and ATR-dependent manner and even that RBR1 and BRCA1 physically interact (Lang et al., 2012; Horvath et al., 2017; Biedermann et al., 2017). Moreover, RBR1 also partially co-localizes at DNA break sites with RADIATION SENSITIVE 51 (RAD51), a recombinase involved in homology-dependent DNA repair (Biedermann et al., 2017). However, the functional relevance for genome integrity of the specific association of RBR1 with DNA repair proteins remains to be elucidated. Notably, RBR1 silencing leads to the upregulation of several

genes involved in DDR and at least for *BRCA1,* RBR1 represses its expression through the DNA-binding of the E2FA transcription factor (Horvath et al., 2017).

Here we show that the F-box protein FBL17 previously reported for its functions in cell cycle regulation, is also involved in DNA damage and repair processes. *FBL17* loss-of-function is associated with a constitutive activation of DDR gene expression, a higher frequency of DNA lesions and increased cell death in the root meristem even in absence of genotoxic stress. Moreover, the *FBL17* mutation leads to hypersensitivity to DSB-induced genotoxic stress. Notably the FBL17 protein is recruited at nuclear foci upon DSB induction and co-localizes with γH2AX. The possible roles of FBL17 in DNA damage-signalling or repair are discussed.

RESULTS

The *fbl17* mutant transcriptome exhibits a strong upregulation of genes related to DNA damage and repair processes

Previous analyses have shown that Arabidopsis *fbl17* mutation leads to reduced leaf size, the appearance of serrated leaves and sterility, likely caused by multiple cell cycle defects (Noir et al., 2015). To further investigate the molecular basis of this phenotype, we performed a RNA sequencing (RNA-seq) analysis based on three biological replicates to identify differentially expressed (DE) genes between Col-0 and *fbl17*-1 homozygous seedlings (Figure 1A; Supplemental Table 1). A global analysis of this data considering all the observed absolute value of log_2FC (i.e. from 0,2 to 6), reveals 6804 DE genes in the *fbl17* mutant compared to the Col-0 genotype (i.e. ~ 25% of the whole transcriptome; Figure 1A). In this analysis, almost 54% of the DE genes in *fbl17* exhibit an upregulated expression level, 46% being down-regulated (Figure 1A). Considering all DE genes in *fbl17*, a Gene Ontology (GO) term enrichment analysis, based on Biological Process functional categories of the ShinyGo software, revealed that genes which expression is widely altered in the mutant are involved in primary metabolic pathways such as the photosynthesis, and other cellular responses, most of them being related to stress conditions (Supplemental Table 2), in line with the severe global phenotypic alterations of the mutant plants.

Remarkably, by filtering DE genes based on Fold Change (i.e. log_2FC absolute value > 1,5; Figure 1B), the comparative RNA-seq analysis revealed that still more than 1400 genes are DE in *fbl17* mutant and their GO term enrichment analysis highlighted their implication in cell cycle progression, DNA replication mechanisms, chromosome dynamics and, in an unexpectedly extended manner, also DNA repair and stress response. This latest category represents 59% of the DE genes exhibiting a log_2FC absolute value > 1,5 (Figure 1B,

Supplemental Figure 1). Among them, 405 genes (*ca.* 79%) exhibit an up-regulation suggesting a constitutive induction of genes linked to DNA damage and stress response. More precisely, using the KEGG (Kyoto Encyclopedia of Genes and Genomes, Kanehisa, et al., 2017) function of the ShinyGO software, six enriched pathways were identified (Supplemental Table 3). One corresponds to the pyrimidine metabolism, involving modifications of both DNA and RNA nucleic acids. The five others are related to DNA metabolism and in particular to DNA replication and DNA repair mechanisms, including mismatch repair, homologous recombination, nucleotide excision repair and base excision repair. Remarkably, in the 6 enriched pathways, the identified genes are all up-regulated in *fbl17*-1 compared to Col-0.

Finally, to validate the RNAseq approach, genes implicated in distinct DNA damage pathways, suggested by the KEGG analysis and some other genes, have been selected and their expression was monitored for comparison by quantitative RT-PCR (RT-qPCR) under standard culture condition in wild-type Col-0, and the *fbl17*-1 homozygous mutant as well as in the KRP2 overexpressor line ($KRP2^{OE}$, Noir et al., 2015) (Figure 1C). The 22 tested genes revealed all the same tendency in terms of expression levels in both analyses, comfortingly validating the data of the RNAseq analysis. Furthermore, besides the expression of *BRCA1, WEE1, ATR, CDKB1;1* and *CYCB1;1* already reported (Noir et al., 2015), the selected genes, *PARP2, RAD51A, MSH4*, *MSH5, RPA1E, PCNA1* and *POL2A* are also upregulated under standard growth condition in *fbl17* but not in the control Col-0 (Figure 1C). Given that *fbl17* mutants present an accumulation of the CDK inhibitor KRP2, it is expected that the $KRP2^{OE}$ line might mimic some of the *fbl17* mutant phenotypes (Noir et al., 2015). Interestingly, in this analysis $KRP2^{OE}$ line exhibits a quite similar pattern to the Col-0 indicating that the constitutive upregulation of DDR genes in *fbl17* is not a direct consequence of KRP2 overaccumulation. Altogether, this analysis indicates that loss of *FBL17* function shows a constitutive and rather global induction of the DDR.

fbl17 mutants reveal an increased frequency of DNA lesions

The constitutive transcriptional DDR suggests that *fbl17* mutants are subjected to genome instability, which is further supported by the occurrence of micronuclei and chromosome bridges previously observed in dividing mutant cells (Noir et al., 2015). To further investigate this issue, we used the sensitive and highly specific γH2AX marker, which detection by immunolabelling can reveal DNA break sites (Figure 2A). Interestingly, the accumulation of γH2AX foci in the *fbl17* mutant background was observed. More precisely, while the frequency of root nuclei exhibiting constitutive γH2AX foci in *fbl17* is only slightly increased

in comparison to Col-0 (i.e. around 20% and 30%, respectively; Figure 2A), the number of γH2AX-marked foci per nucleus can reach a much higher amount in *fbl17* than in Col-0 nuclei (Figure 2B), reflecting an excessive frequency of DNA lesions even in absence of genotoxic stress.

fbl17 mutants are hypersensitive to drug inducing DSB DNA lesions

Given the specificity of the γH2AX recruitment at DNA lesion sites and their accumulation in the *fbl17* loss-of-function mutant, also considering that this type of DNA lesions can especially result in loss of genetic information, a special interest was given to genotoxic conditions triggering DSB DNA lesions. In a first step, transcript levels of the previously tested DNA damage genes were evaluated after the treatment of seedlings with zeocin, an antibiotic of the bleomycin (BLM) family widely used as an inducer of DSBs. It should be mentioned that the *FBL17* gene is not itself differentially regulated neither upon genotoxic stress nor in the tested DDR mutant background *sog1*-1 (Figure 3). Under zeocin treatment, a number of genes known to be involved in DDR pathways, such as *RAD51A, TSO2, BRCA1, SMR7, GR1, RPA1E, RAD17, PARP2, XRI1, SYN2, CYCB1;1, SIP4,* among others, appear strongly induced in the control Col-0 (Figure 3B). According to the literature, many of these genes are known to be induced after DSB-inducing stress, being targeted by the transcription factor SOG1 (Culligan et al., 2006); (Ogita et al., 2018). Notably, for several of them such as *RAD51A, BRCA1, SMR7*, *PARP2* and *XRI1,* while they are also induced in *fbl17*, their induction level is less intense compared to the Col-0 control, possibly due to the pre-existing constitutive induction of these genes in the mutant (Figure 3A). In addition, *TSO2, NSE4, GR1*, *TIL1*, *RPA1E, WEE1, RPA70C* and *RAD17* did not appear to be induced by zeocin in *fbl17*, likely because they have already reached their maximal gene expression level in the mutant even in the absence of the drug. Lastly, some genes (i.e. *LIG4, PCNA1, FAN1, ATM* and *ATR* ; Supplemental Figure 2) were not upregulated after zeocin treatment neither in the *fbl17* mutant nor in the control. This is in accordance with previous analyses showing that these genes are not induced by DSB stress and are not targeted by SOG1 (Culligan et al., 2006).

Next, we investigated the sensitivity of the *fbl17* mutant to zeocin treatment using a root elongation assay. As already observed, the severe delay of *fbl17* primary root elongation was confirmed under standard condition (Figure 4A). The *atm-2* mutant was used as a sensitive control (Garcia et al., 2003) and as expected after 4 days upon zeocin treatment, the primary root elongation of this mutant started to be slightly delayed (Figure 4A), confirming the efficacy of the treatment. At the same time point, Col-0 and KRP2^{OE}, were not yet affected by the

chemical treatment, while *fbl17* root elongation completely stopped already at day 3. After 7 days of zeocin treatment, *atm-2* exhibits an intermediate phenotype of root length inhibition (i.e. 40%, median value), between the respective ratios of around 5-6% for the Col-0 and KRP2^{OE}, and 60% for the *fbl17* mutant line (Figure 4B).

A strategy undertaken by multicellular organisms to eliminate damaged cells is to actively trigger cell death (Hu et al., 2016). Using the same experimental culture conditions, occurrence of cell death was estimated after 3 days of zeocin exposure. As expected, the *atm-2* sensitive mutant exhibits more cell death than the control Col-0 (Fulcher and Sablowski, 2009) and the KRP2^{OE} line. Remarkably, while *fbl17* root tips already exhibit constitutive cell death, a further accumulation is noticed upon zeocin treatment, which corresponds to an even higher number of dead cells than observed in *atm-2* mutant (Figures 4C and 4D). In addition, whereas cell death observed in Col-0 root tips is qualitatively mainly located at the level of the quiescent centre (QC), cell death in *fbl17* occurs at the QC level as well as in more distant tissues of the root. Finally, the frequency of γH2AX foci was monitored after zeocin treatment in Col-0 and *fbl17* (Figure 2A). Under this condition, the frequency of γH2AX-marked nuclei in *fbl17* (*ca.* 70%) becomes significatively higher than in Col-0 (*ca.* 30%; Figure 2B). Moreover, γH2AX-marked nuclei accumulate a larger number of foci per nucleus in *fbl17*, with in some of them more than 20 γH2AX foci observed in one nucleus.

Altogether, the impaired root meristem activity, the accumulation of cell death and the increased number of γH2AX foci upon zeocin treatment, argue that the *fbl17* mutant is hypersensitive to DSB-induced genotoxic stress. This phenotype is not the consequence of KRP overaccumulation occurring in *fbl17* mutants, but rather suggests that FBL17 might be involved in DDR beyond its cell cycle regulatory functions.

The constitutive overexpression of DDR genes in *fbl17* and its hypersensitivity to DSB inducer is SOG1-independant

Mechanisms sensing DNA lesions and initiating DDR involve massive gene regulation ultimately leading to DNA repair. At this control level, the Arabidopsis SOG1 transcription factor of the NAC family has been shown to be a master regulator controlling multiple DDR pathways (Yoshiyama, 2016)(Ogita et al., 2018)(Bourbousse et al., 2018). As already mentioned above (see Figure 3), *SOG1* is not differentially regulated in *fbl17* at transcriptional level. In order to investigate the putative implication of SOG1 in the DDR observed in *fbl17* mutant, the double mutant *fbl17-1 sog1-1* has been generated. At a macroscopic level, the developmental phenotype of the double mutant was similar to the *fbl17* single mutant

(Supplemental Figure 3). Though, regarding its root growth, the double mutant exhibits a minor rescue of the root length (Figure 4A). Upon genotoxic stress, while *sog1-1* exhibits a slight resistance to zeocin in our experimental conditions (Figure 4B; see also Adachi et al., 2011), the *fbl17-1 sog1-1* double mutant shares a similar level of sensitivity with the *fbl17* single mutant when tested both for root growth inhibition (Figure 4B) and for cell death occurrence (Figures 4C-D). Despite the absence of obvious rescue of the *fbl17* phenotype by the *sog1* mutation, we next asked whether *SOG1* loss-of-function could at least partially attenuate the global up-regulation of DNA damage genes observed in the *fbl17* mutant background.

At first, by testing some gene-targets of SOG1 not implicated in DDR according to Ogita et al. (2018), we could verify that those genes (e.g. *EDA18, KRP6, SAG101, BRL3, AGO2*) are not constitutively up-regulated in the *fbl17* single mutant and as expected in *fbl17-1 sog1-1* (Figure 3A). Nevertheless, most of the DDR genes constitutively induced without genotoxic stress were similarly differentially expressed in *fbl17-1 sog1-1* as in the *fbl17* single mutant (Figure 3A), with the exception of *TSO2* and *SMR7* showing only a slight decrease of expression. In contrast and as expected, the induction by zeocin of these genes is fully suppressed in the *sog1-1* single mutant and also in the *fbl17-1 sog1-1* double mutant (Figure 3B). It is however noteworthy that upon zeocin treatment, only the additive increase of expression of some DDR genes in *fbl17* (e.g. *RAD51A*, *BRCA1*, *SMR7, PARP2*) is dependent on SOG1. Altogether these results indicate that the constitutive DDR and the hypersensitivity to DSB-induced genotoxic stress observed in *fbl17* does not depend on SOG1, but likely other transcriptional regulatory mechanisms.

FBL17 is recruited at nuclear foci upon DSB induction

It was previously shown that FBL17 is a nuclear F-box protein restricted to few cells in the root meristem, showing a cell cycle phase-dependent expression pattern (Noir et al., 2015)(Desvoyes et al, 2019 BioRXiv ID). We next investigated whether DNA damage affects the subcellular distribution of FBL17. To answer to this question, we took advantage of the previously established *fbl17-1*, pFBL17:FBL17-GFP seedlings (Noir et al., 2015). At first, the sensitivity to zeocin of this reporter line was monitored using the root elongation assay (Supplemental Figures 4A, B) and by RT-qPCR analysis (Supplemental Figures 4D). In the tested conditions, the reporter line exhibited a similar behavior as the Col-0 wild-type control supporting that the FBL17-GFP protein is functional and can confidently be used for our analyses. Consequently, the GFP-reporter line was exposed to distinct genotoxic stresses and the distribution of the fusion protein was imaged by confocal microscopy (Figure 5A). For this

assay we used zeocin to induce DSB DNA lesions, and due to the implication of FBL17 in DNA replication, cisplatin and hydroxyurea (HU) treatments were also applied to trigger DNA crosslinking and stalled replication forks, respectively. Under these conditions, at a tissue level no obvious differential distribution of the FBL17-GFP protein was observed between the 3 treatments tested. However, focusing at a subcellular nuclear level, the formation of FBL17 nuclear foci could be observed only with the zeocin treatment, but neither with cisplatin nor HU, suggesting that the formation of FBL17 foci might be specific to DSB-type of DNA lesions.

DSB-type of DNA lesions recruit FBL17 at γH2AX foci

The observation of FBL17 foci upon genotoxic stress was reminiscent of the γH2AX foci formation. Intriguingly it was recently shown that besides the expected proteins from the DNA damage machinery, two cell cycle transcriptional regulator, the E2FA transcription factor and RETINOBLASTOMA RELATED 1 (RBR1) also localized at DNA damage sites in Arabidopsis (Lang et al., 2012)(Horvath et al., 2017)(Biedermann et al., 2017). To better define the FBL17 foci, we used an immunostaining approach which despite revealing a low frequency of nuclei with FBL17 foci (Supplemental Table 5), allowed us to investigate whether they co-localize with γH2AX foci and/or RBR1. Indeed, we observed the co-localization of FBL17 with γH2AX foci in some nuclear foci supporting the recruitment of the F-box protein at DNA lesion sites upon zeocin treatment (Figure 5B). More interestingly, we also observed a clear colocalization of FBL17 and RBR1 (Figures 5B and 5C). In fact, quantification of these nuclear foci under zeocin treatment, revealed a mean value of 5% of colocalization of RBR1 with γH2AX and 5% of colocalization of FBL17 with RBR1 (Figure 5D and Supplemental Table 5). Note that FBL17 and γH2AX never colocalize if RBR1 is not itself detected at these foci (Figure 5D and Supplemental Table 5) and co-localization of all three proteins together represented only 1% of our observations. These results suggest that FBL17 and RBR1 follow a dynamic recruitment at the DNA damage sites, were they likely contribute to DNA repair and genome integrity.

DISCUSSION

We have previously shown that loss of function of Arabidopsis *FBL17* slows plant growth by decreasing cell proliferation and also suppresses endoreplication (Noir et al., 2015). At the molecular level, *fbl17* mutant plants showed increased accumulation of the KRP2 protein, known to switch off CDKA;1 kinase activity (Verkest et al., 2005), and phenotypically resemble the *cdka;1* null mutant (Nowack et al., 2012), indicating that a main function of FBL17 is to positively regulate CDKA;1 activity. In line with such a role, the loss of *FBL17* delayed or even blocked S-phase in some cells and led to the differential expression of cell cycle genes and consistently among them genes involved in the process of DNA replication (Noir et al., 2015). However, our transcriptomic approach revealed that the *fbl17* mutation also leads to a broader activation of numerous DNA damage and repair genes beyond those solely linked to DNA replication stress. Note that genome wide transcriptional studies of synchronized plant cells revealed that several DDR genes have their expression maximum in S-phase (Menges et al., 2005)(Trolet et al., 2019).

In plants, a major regulator of the DDR is the transcription factor SOG1, which has been functionally compared to the mammalian tumour suppressor p53 (Yoshiyama et al., 2009)(Yoshiyama, 2016). SOG1 is directly phosphorylated by ATM and its mutation impairs DNA repair, cell cycle arrest, and activation of cell death (Preuss and Britt, 2003)(Yoshiyama et al., 2009)(Furukawa et al., 2010). According to our analysis, FBL17 does however not seem to act at the level of SOG1. First, the constitutive transcriptional activation of DDR genes in *fbl17* is not suppressed by the *sog1* mutation. Second, many of the SOG1 target genes can still be induced upon zeocin treatment in the *fbl17* mutant background. Third, the hypersensitivity of *fbl17* mutants to DSB inducing agents as well as the increase in the amount of cell death is not dependent on SOG1.

Interestingly, it has recently been shown that several genes involved in DNA damage repair are induced when RBR1 is down-regulated by RNAi or in the hypomorphic *rbr1-2* mutant (Biedermann et al., 2017)(Horvath et al., 2017). At least for Arabidopsis *BRCA1*, it was shown that RBR directly represses this gene through the E2FA transcription factor (Horvath et al., 2017). A genome-wide RBR1-ChIP analysis further indicated that RBR1 is recruited to E2F-sites present in the promoter of many DDR genes (Bouyer et al., 2018). According to our analysis combining the information of E2FA-binding sites (Verkest et al., 2014) with the RBR1-ChIP dataset (Bouyer et al., 2018), several of the DDR genes constitutively induced in *fbl17* are likely targets of RBR/E2FA.

At the functional level, it was reported that *rbr1* mutants exhibit an elevated level of DNA damage in normal growth conditions, while after BLM-treatment, these mutants had a

significantly higher level of DNA fragmentation (Biedermann et al., 2017)(Horvath et al., 2017). Moreover, both the lack of functional RBR1 and the loss of E2FA resulted in hypersensitivity against DNA DSB-inducing agents (Biedermann et al., 2017) (Roa et al., 2009)(Lang et al., 2012). Thus, the loss of *FBL17* function shares many similarities with the phenotype of RBR/E2FA-deficient plants suggesting that the F-box protein could act at this level. Indeed, we observed the colocalization of FBL17 and RBR at DNA damage sites. The recruitment of RBR1 and E2FA to γH2AX foci has been previously reported (Lang et al., 2012)(Biedermann et al., 2017)(Horvath et al., 2017), suggesting that these proteins might play a more direct role in DNA repair besides their known transcriptional regulatory function. Interestingly, RBR1 co-localizes with the RADIATION SENSITIVE 51 (RAD51) protein and is necessary for RAD51 localization to DNA after BLM treatment (Biedermann et al., 2017). RBR1 also co-localizes with BRCA1 foci upon DNA stress, although RBR1 recruitment to γH2AX foci was found independent of BRCA1 (Horvath et al., 2017). As shown in mammals, where Rb physically interacts with the BRCA1 (Aprelikova et al., 1999), RBR1 also directly interacts with BRCA1 in plants (Horvath et al., 2017), suggesting a structural role of the Retinoblastoma in the DNA damage repair machinery. Our observation that FBL17 and RBR1 co-localize in nuclear foci after DNA damage generating DSBs, suggests that the F-box protein directly participates in the process of DNA repair. Since FBL17 association with γH2AX seems to depend on RBR1, it is possible that the later recruits FBL17 at the DNA damage sites in a dynamic manner. This raises the question of which proteins might be ubiquitylated by FBL17 at the sites of DNA lesions.

In mammalian cells, DSB repair implies a complex interplay between ubiquitylation and SUMOylation for a faithful repair of such damage (Schwertman et al., 2016). In particular it has been shown that ubiquitylation of proteins in the vicinity of DNA lesions functions as a recruitment signal for DSB repair factors. Ubiquitylation and deubiquitylation cycles also control the steady state level of DSB repair factors and/or their interactions. Of particular interest for our study is the mammalian F-box protein Skp2. While Skp2 is a main regulator of the cell cycle (Frescas and Pagano, 2008)(Starostina and Kipreos, 2012), it has also been involved in DDR. Thus, it was shown that Skp2 is required for the activation and recruitment of the ATM kinase to DNA damage foci (Wu et al., 2012). At the molecular level, in response to DSBs Skp2 triggers the K63-dependent ubiquitylation of NBS1, a component of the MRN complex, which in turn facilitates ATM recruitment to the DNA foci for activation. Skp2 ubiquitylates also other proteins at DSBs such as BRCA1, which seems important for the timing of end resection (Parameswaran et al., 2015). Similarly to Skp2, the Arabidopsis FBL17 F-box

protein is able to degrade CKI proteins ((Noir et al., 2015) and references therein), but whether it also ubiquitylates components of the DNA repair machinery is presently unknown. Note that at the DNA damage sites, RBR itself and/or E2FA are also possible candidate substrates of the SCF^{FBL17} ubiquitin E3 ligase. Therefore, further experiments will be necessary to elucidate the function of this plant F-box protein at DSB sites.

MATERIALS AND METHODS

Plant Material

The following *Arabidopsis* lines were used in this study : the T-DNA insertion lines *fbl17-1* (Gabi-KAT_170-E02; (Noir et al., 2015), *atm-2* (SALK_006953; (Garcia et al., 2003)), the EMS mutant line *sog1-1* (Yoshiyama et al., 2009) and the Arabidopsis reporter and/or overexpressor lines *fbl17-1*, pFBL17:FBL17-GFP, 35S:FBL17-GFP and GFP-KRP2OE described in Noir et al (2015). T-DNA insertions and mutations were confirmed by PCR-based genotyping and by further sequencing for the *sog1-1* allele. The *fbl17-1 sog1-1* double mutant was generated by performing crosses and genotyping/sequencing of the resulting F2 and/or F3 progenies by PCR-based approaches. Primers designed for this purpose are listed in Supplemental Data (Supplemental Table 4).

Plant Growth Conditions

For *in vitro* growth conditions, seed sterilization, stratification and *in vitro* culture were performed as described in (Noir et al., 2015) with or without supplemented genotoxic agent. To obtain flowering plants and seeds, seedlings initially grown under *in vitro* culture were transferred on soil at day 6-8 and kept in 16-h-light/8-h-dark growth chambers under fluorescent light (Osram Biolux 49W/965).

For the monitoring of root growth, seedlings were germinated and grown *in vitro* on vertical plates using 1% agar MS medium and transferred at day 5 on 1% agar MS medium without or with 5 µM zeocin (Invitrogen). Root elongation was scored each day for 7 days and root length was measured using Fiji software (ImageJ 1.52p; http://imageJ.nih.gov/ij). The final values were calculated by determining the arithmetic mean of the root length values of three biological replicates, which were themselves the average of 4 to 37 plants using the R software (version 3.6.1).

Quantitative RT-PCR analysis

The purification of total RNAs from 8 day-old seedlings grown under *in vitro* conditions was performed using Tri-Reagent (Molecular Research Center, Inc) according to the manufacturer's instructions. cDNAs were prepared using the High Capacity cDNA Reverse Transcription Kit (Applied Biosystems). Real-time amplification was performed using gene-specific primers and SYBR Green Master Mix (Roche) on a LightCycler LC480 apparatus (Roche) according to the manufacturer's instructions. The mean value of three replicates was normalized using the TIP4.1 (AT4G34270) and SAND (AT2G28390) genes as internal controls. All primers used in quantitative RT-PCR are listed in Supplemental Table 4.

Nucleic acid isolation, cDNA library preparation, sequencing and data analysis

Total RNAs were extracted by using Trizol solution (Invitrogen) from 10 day-old *fbl17*-1 and Col-0 seedlings grown *in vitro* as described above completed by a second phenol/chloroform treatment. Three biological replicates were used as starting material. RNAs concentrations were determined with a QuBit Fluorometer (Thermo Fisher Scientific). RNAs integrities were checked using the 2100 Bioanalyzer (Agilent). mRNAs were isolated from total RNAs by using the NEBNext® Poly(A) mRNA Magnetic Isolation Module (NEB) for mRNA libraries preparation. Sequencing libraries were prepared using the Collibri stranded RNA library kit for Illumina (Invitrogen). The libraries were sequenced using an Illumina Nextseq 500 system (single-end mode 1 × 75 bp).

For the bioinformatics analysis, the pre-processing of the sequencing data was performed using TrimGalore (v0.5.0; https://www.bioinformatics.babraham.ac.uk/projects/trim_galore): reads were processed by removing the adaptor sequences using Cutadapt v1.18 and quality was assessed using FastQC v0.11.8 (https://www.bioinformatics.babraham.ac.uk/projects/fastqc/). The reads with quality > 30 and minimal read length of 50 pb were kept. The data were mapped to the *Arabidopsis thaliana* genome (TAIR10) using Hisat2 (v2.1.0) software (Kim et al., 2015) and sorted with Samtools v1.9 (Li et al., 2009). For each gene, read quantification was performed using the HTSeq-count v0.11.0 software (with parameter "intersection nonempty") (Anders et al., 2015). Differential expression analysis by pairwise comparison has been performed using the R package DESeq2 (v1.24.0) (Anders and Huber, 2010) and betaprior parameter set to true. Gene Ontology and KEGG enrichment analysis were performed using ShinyGo v0.61 software (Ge and Jung, 2018 bioRxiv).

Immunolabelling

Fixation and immunostaining were performed as previously described (Batzenschlager et al., 2015) from 6 day-old *in vitro* grown seedlings. The primary antibodies used were the rabbit polyclonal anti-γH2AX (diluted at 1/500; provided by Davids biotechnologie (Regensburg, Germany) against the synthetic phosphopeptide VGKNKGDIGSA(p)SQGEF as described in Friesner et al., 2005 Mol Biol Cell. 2005 May; 16(5): 2566–2576.), the mouse monoclonal anti-GFP (1/500; Life Technologies) and the chicken polyclonal anti-RBR1 (1/7000; Agrisera). Depending on the experiments, the conjugated-secondary antibodies for γH2AX detection were either the goat anti-rabbit Alexa Fluor 568 (1/300; Life Technologies) for red signals or the goat anti-rabbit Cyn5 (1/500; Life Technologies) for purple signals. For GFP and RBR1 detection, the conjugated secondary antibodies used were, respectively, the goat anti-mouse Alexa Fluor 488 (1/200; Interchim) for the green signal and, the goat anti-chicken Alexa Fluor 568 (1/300; Life Technologies) for red signal.

Confocal Microscopy Analyses and Image Treatments

All confocal microscopy observations were performed by using the Leica TCS SP8 microscope. Roots of seedlings expressing fluorescent reporter constructs were observed after treatment upon 20 µM zeocin (Invitrogen), 15 µM cisplatin (Sigma) or 5 mM hydroxyurea (Sigma) or after transfer under standard condition for 16 h, and just before observation, were counterstained in 75 mg/mL propidium iodide (Fluka). To score cell death, 8 day-old seedlings not treated or treated for 3 days under 5 µM zeocin were stained as described in (Biedermann et al., 2017). Dead cell quantification was performed at the quiescent centre (QC) plan considering a fixed area of 15000 μm^2 (200 µm-length from the QC towards the elongation zone on 75 µm-width) using Fiji software (ImageJ 1.52p; http://imageJ.nih.gov/ij). The final values were calculated by determining the arithmetic mean of three biological replicates ($4 < N$ per genotype < 11) using the R software (version 3.6.1). For immunolabelling imaging, confocal images of fixed nuclei were taken as a consecutive series along the Z-axis. Microscope settings were kept the same for image acquisition of each genotype and/or condition, and signal colocalization was evaluated using the Fiji software.

Accession Numbers

The accession numbers of the main genes mentioned in this study are as follows:
AT3G54650 (*FBL17*), AT1G25580 (*SOG1*), AT3G48190 (*ATM*), AT5G40820 (*ATR*), AT4G21070 (*BRCA1*), …

ACKNOWLEDGMENTS

We thank Jérôme Mutterer from the IBMP Microscopy and Cellular Imaging platform for confocal microscopy support, Sandrine Koechler and Abdelmalek Alioua from the IBMP Gene Expression Analysis platform as well as Anne Molitor, Antoine Hanauer and Raphael Carapito from the GENOMAX platform of INSERM UMRS_1109 for Next-Generation Sequencing experiments.

This work was supported by the Grand-Est Region (N° 168947), the Agence Nationale de la Recherche-PRCI program ANR-RHiD "ANR-19-CE13-0032" and the LABEX program "ANR-10-LABX-0036_NETRNA."

FIGURE LEGENDS

Figure 1. The whole transcriptome of the *fbl17* mutant reveals misexpression of numerous cell cycle and DNA damage/repair genes.

(A) All differentially expressed (DE) genes in *fbl17* compared with Col-0 wild type plants (log_2 fold-change; x-axis) were plotted against the -log_{10}(adjusted p-value). The horizontal line indicates the significance threshold for DE genes (p-value <0.05). Up- and down- regulated genes are shown with green and orange dots, respectively. Non-differentially expressed genes are shown with grey dots.

(B) Gene Ontology (GO) functional analysis of DE genes in *fbl17* exhibiting a log_2FC absolute value > 1,5 (i.e. 1443 genes). The GO enrichment analysis is based on Biological Process functional categories of the ShinyGo v0.61 software. The 5 major functional groups are based on the 50 most significant terms taken account from the hierarchical clustering tree summarizing the correlation among pathways with many shared genes (Supplemental Figure 1). The number of non-redundant genes (n) per functional group and the corresponding percentage are indicated in brackets.

(C) Relative expression levels of gene transcripts from 8 day-old *in vitro* grown plants of the indicated genotype were determined by RT-qPCR. The bar graph depicts expression level mean values of the indicated transcripts of one independent replicate (±SE of the technical triplicate). The experiment was repeated two times giving the same tendency.

Figure 2. Increased accumulation of γH2AX foci in *fbl17*.

(A) Representative images of Col-0 and *fbl17-1* after immunostaining of γH2AX foci (red) in root tip nuclei from seedlings not treated or treated for 16 h with zeocin (5µM). Nuclei were counterstained with DAPI (blue). Scale bar = 2 µm.
(B) Quantification of γH2AX foci in Col-0 and *fbl17*-1 nuclei from Col-0 and *fbl17-1* seedlings not treated or treated with zeocin. Between 79 and 233 nuclei per line per replicate were analysed and categorised into six types (no γH2AX, 1–2, 3–5, 6–10, 11–20, or more than 20 γH2AX foci/nuclei, respectively). Two independent replicates were performed. Error bars indicate the standard deviation.

Figure 3. DDR gene expression levels during zeocin treatment in Col-0 and *fbl17, sog1* single and double mutant backgrounds.
(A) Relative expression levels of gene transcripts in 8 day-old *in vitro* grown plants of the indicated genotypes were determined by RT-qPCR.
(B) Relative expression levels of gene transcripts in 8 day-old *in vitro* grown plants of the indicated genotypes after 3 hours of 20 µM zeocin treatment were determined by quantitative RT-qPCR.
(A,B) The bar graph depicts expression level mean values of the indicated transcripts of one independent replicate (±SE of the technical triplicate). The experiment was repeated two times giving the same results.

Figure 4. The *fbl17* mutant exhibits hypersensitivity to zeocin treatment.
(A) Root growth elongation of the indicated genotypes of 5 day-old seedlings grown under standard condition and transferred on medium not supplemented (**upper panel**) or containing 5 µM zeocin (**lower panel**) for further 7 days of culture. Error bars indicate the standard deviation of the mean value of three independent experiments (4 <N per genotype < 37). The asterisks indicate a p-value <0,05(*), <0,01(**) and <0,001(***) in Wilcoxon-Mann-Whitney test between *fbl17*-1 and *fbl17*-1 *sog1*-1. Complete statistical analysis is given in the Supplemental Table 4.
(B) Percentage of root length inhibition for the experiment described in (A). Significance statistical analysis has been calculated by Wilcoxon-Mann-Whitney test. Box whiskers with different letters (a, b, c, d and e) denote statistical differences (one-way analysis of variance, p < 0,05 at least). Complete statistical analysis is given in the Supplemental Table 4.
(C) Representative images of root tips of 5-day old seedlings transferred on medium not supplemented (control) or containing 5 µM zeocin for further 3 days of growth before

propidium iodide staining. Scale bars = 50 µm. Three independent replicates were performed (4 < N per genotype < 11).

(D) Cell death quantification of the root samples illustrated in (C) on medium not supplemented (-) or containing 5 µM zeocin (+) for further 3 days. Significance statistical analysis has been calculated by Wilcoxon-Mann-Whitney test. Box whiskers with different letters (a, b, c, d and e) denote statistical differences (one-way analysis of variance, $p < 0,05$ at least). Complete statistical analysis is given in the Supplemental Table 4.

Figure 5. FBL17 proteins are recruited at γH2AX foci and colocalize with RBR1 upon DSB-inducer stress.

(A) Live microscopy on *fbl17*-1, pFBL17:FBL17-GFP after 16 hours upon genotoxic treatment (zeocin 20 µM, cisplatin 15 µM or hydroxyurea 5 mM). Scale bars = 50 µm (**upper panel**) and 2 µm (**lower panel**). Three independent experiments were analysed (5 <N per genotype < 10).

(B) Representative images of *fbl17*-1, pFBL17:FBL17-GFP root nuclei with triple immunolocalization of γH2AX (purple), RBR1 (red) and FBL17-GFP (anti-GFP, green) showing co-localisation of the 3 signals after 16 h of zeocin treatment (20µM) highlight by arrowheads. Nuclei were counterstained with DAPI (blue). Scale bar = 2 µm.

(C) Signal intensity distribution of the total amount of pixels at the X-axis shown in zeocin-treated nucleus in (B). Statistical significance analysis of the signal colocalisation is given in the Supplemental Table 4.

(D) Venn diagram showing the frequency of the different colocalization combinations of FBL17-, RBR1- and γH2AX-foci in the nuclei of one replicate (total number of foci = 758). Complete frequency analysis of the three independent replicates is given in the Supplemental Table 5.

REFERENCES

Adachi, S. et al. (2011). Programmed induction of endoreduplication by DNA double-strand breaks in Arabidopsis. Proc. Natl. Acad. Sci. **108**: 10004–10009.

Amiard, S., Gallego, M.E., and White, C.I. (2013). Signaling of double strand breaks and deprotected telomeres in arabidopsis. Front. Plant Sci. **4**: 1–6.

Anders, S. and Huber, W. (2010). Differential expression analysis for sequence count data. Genome Biol. **11**: R106.

Anders, S., Pyl, P.T., and Huber, W. (2015). HTSeq-A Python framework to work with high-throughput sequencing data. Bioinformatics **31**: 166–169.

Aprelikova, O.N., Fang, B.S., Meissner, E.G., Cotter, S., Campbell, M., Kuthiala, A., Bessho, M., Jensen, R.A., and Liu, E.T. (1999). BRCA1-associated growth arrest is RB-dependent. Proc. Natl. Acad. Sci. U. S. A. **96**: 11866–11871.

Batzenschlager, M. et al. (2015). Arabidopsis MZT1 homologs GIP1 and GIP2 are essential for centromere architecture. Proc. Natl. Acad. Sci. U. S. A. **112**: 8656–8660.

Biedermann, S., Harashima, H., Chen, P., Heese, M., Bouyer, D., Sofroni, K., and Schnittger, A. (2017). The retinoblastoma homolog RBR1 mediates localization of the repair protein RAD51 to DNA lesions in *Arabidopsis*. EMBO J. **36**: 1279–1297.

Bourbousse, C., Vegesna, N., and Law, J.A. (2018). SOG1 activator and MYB3R repressors regulate a complex DNA damage network in Arabidopsis. Proc. Natl. Acad. Sci. **115**: E12453–E12462.

Bouyer, D., Heese, M., Chen, P., Harashima, H., Roudier, F., Grüttner, C., and Schnittger, A. (2018). Genome-wide identification of RETINOBLASTOMA RELATED 1 binding sites in Arabidopsis reveals novel DNA damage regulators. ref to complete

Cools, T. and De Veylder, L. (2009). DNA stress checkpoint control and plant development. Curr. Opin. Plant Biol. **12**: 23–28.

Culligan, K.M., Robertson, C.E., Foreman, J., Doerner, P., and Britt, A.B. (2006). ATR and ATM play both distinct and additive roles in response to ionizing radiation. Plant J. **48**: 947–961.

Denicourt, C. and Dowdy, S.F. (2004). Cip/Kip proteins: More than just CDKs inhibitors. Genes Dev. **18**: 851–855.

Dickey, J.S., Redon, C.E., Nakamura, A.J., Baird, B.J., Sedelnikova, O.A., and Bonner, W.M. (2009). H2AX: Functional roles and potential applications. Chromosoma **118**: 683–692.

Feldman, R.M.R., Correll, C.C., Kaplan, K.B., and Deshaies, R.J. (1997). A complex of Cdc4p, Skp1p, and Cdc53p/cullin catalyzes ubiquitination of the phosphorylated CDK inhibitor Sic1p. Cell **91**: 221–230.

Frescas, D. and Pagano, M. (2008). Deregulated proteolysis by the F-box proteins SKP2 and β-TrCP: Tipping the scales of cancer. Nat. Rev. Cancer **8**: 438–449.

Fulcher, N. and Sablowski, R. (2009). Hypersensitivity to DNA damage in plant stem cell niches. Proc. Natl. Acad. Sci. **106**: 20984–20988.

Furukawa, T., Curtis, M.J., Tominey, C.M., Duong, Y.H., Wilcox, B.W.L., Aggoune, D.,

Hays, J.B., and Britt, A.B. (2010). A shared DNA-damage-response pathway for induction of stem-cell death by UVB and by gamma irradiation. DNA Repair (Amst). **9**: 940–948.

Garcia, V., Bruchet, H., Camescasse, D., Granier, F., Bouchez, D., and Tissier, A. (2003). AtATM is essential for meiosis and the somatic response to DNA damage in plants. Plant Cell **15**: 119–132.

Ge S. X., and Jung D. (bioRxiv). ShinyGO: a graphical enrichment tool for animals and plants. http://dx.doi.org/10.1101/315150 doi: bioRxiv preprint first posted online May. 4, 2018;

Gusti, A., Baumberger, N., Nowack, M., Pusch, S., Eisler, H., Potuschak, T., De Veylder, L., Schnittger, A., and Genschik, P. (2009). The Arabidopsis thaliana F-box protein FBL17 is essential for progression through the second mitosis during pollen development. PLoS One **4**.

Horvath, B.M. et al. (2017). Arabidopsis RETINOBLASTOMA RELATED directly regulates DNA damage responses through functions beyond cell cycle control . EMBO J. **36**: 1261–1278.

Hu, Z., Cools, T., and De Veylder, L. (2016). Mechanisms Used by Plants to Cope with DNA Damage. Annu. Rev. Plant Biol. **67**: 439–462.

Huang, D.W., Sherman, B.T., and Lempicki, R.A. (2009). Systematic and integrative analysis of large gene lists using DAVID bioinformatics resources. Nat. Protoc. **4**: 44–57.

Kanehisa M., Furumichi M., Tanabe M., Sato Y., Morishima K. (2017) KEGG: new perspectives on genomes, pathways, diseases and drugs. *Nucleic Acids Res* 2017;45(D1):D353-D361.

Kim, D., Langmead, B., and Salzberg, S.L. (2015). HISAT: A fast spliced aligner with low memory requirements. Nat. Methods **12**: 357–360.

Kim, H.J., Oh, S.A., Brownfield, L., Hong, S.H., Ryu, H., Hwang, I., Twell, D., and Nam, H.G. (2008). Control of plant germline proliferation by SCF FBL17 degradation of cell cycle inhibitors. **455**.ref to complete

Lang, J., Smetana, O., Sanchez-Calderon, L., Lincker, F., Genestier, J., Schmit, A.C., Houlné, G., and Chabouté, M.E. (2012). Plant γH2AX foci are required for proper DNA DSB repair responses and colocalize with E2F factors. New Phytol. **194**: 353–363.

Li, H., Handsaker, B., Wysoker, A., Fennell, T., Ruan, J., Homer, N., Marth, G., Abecasis, G., and Durbin, R. (2009). The Sequence Alignment/Map format and SAMtools. Bioinformatics **25**: 2078–2079.

Malumbres, M. and Barbacid, M. (2005). Mammalian cyclin-dependent kinases. Trends

Biochem. Sci. **30**: 630–641.

Menges, M., De Jager, S.M., Gruissem, W., and Murray, J.A.H. (2005). Global analysis of the core cell cycle regulators of Arabidopsis identifies novel genes, reveals multiple and highly specific profiles of expression and provides a coherent model for plant cell cycle control. Plant J. **41**: 546–566.

Nisa, M., Huang, Y., Benhamed, M., and Raynaud, C. (2019). The Plant DNA Damage Response : Signaling Pathways Leading to Growth Inhibition and Putative Role in Response to Stress Conditions. **10**: 1–12. journal?

Noir, S., Marrocco, K., Masoud, K., Thomann, A., Gusti, A., Bitrian, M., Schnittger, A., and Genschik, P. (2015). The Control of Arabidopsis thaliana Growth by Cell Proliferation and Endoreplication Requires the F-Box Protein FBL17. Plant Cell **27**: 1461–1476.

Nowack, M.K., Harashima, H., Dissmeyer, N., Zhao, X., Bouyer, D., Weimer, A.K., De Winter, F., Yang, F., and Schnittger, A. (2012). Genetic Framework of Cyclin-Dependent Kinase Function in Arabidopsis. Dev. Cell **22**: 1030–1040.

Nurse, P. (2000). A long twentieth century of the cell cycle and beyond. Cell **100**: 71–78.

Ogita, N. et al. (2018). Identifying the target genes of SUPPRESSOR OF GAMMA RESPONSE 1, a master transcription factor controlling DNA damage response in Arabidopsis. Plant J. **94**: 439–453.

Parameswaran, B., Chiang, H.C., Lu, Y., Coates, J., Deng, C.X., Baer, R., Lin, H.K., Li, R., Paull, T.T., and Hu, Y. (2015). Damage-induced BRCA1 phosphorylation by Chk2 contributes to the timing of end resection. Cell Cycle **14**: 437–448.

Preuss, S.B. and Britt, A.B. (2003). A DNA-damage-induced cell cycle checkpoint in arabidopsis. Genetics **164**: 323–334.

Roa, H., Lang, J., Culligan, K.M., Keller, M., Holec, S., Cognat, V., Montané, M.H., Houlné, G., and Chabouté, M.E. (2009). Ribonucleotide reductase regulation in response to genotoxic stress in arabidopsis. Plant Physiol. **151**: 461–471.

Schwertman, P., Bekker-Jensen, S., and Mailand, N. (2016). Regulation of DNA double-strand break repair by ubiquitin and ubiquitin-like modifiers. Nat. Rev. Mol. Cell Biol. **17**: 379–394.

Schwob, E., Böhm, T., Mendenhall, M.D., and Nasmyth, K. (1994). The B-type cyclin kinase inhibitor p40SIC1 controls the G1 to S transition in S. cerevisiae. Cell. to complete

Sjogren, C.A., Bolaris, S.C., and Larsen, P.B. (2015). Aluminum-Dependent Terminal Differentiation of the Arabidopsis Root Tip Is Mediated through an ATR-, ALT2-, and

SOG1-Regulated Transcriptional Response. Plant Cell **27**: 2501–2515.

Spampinato, C.P. (2017). Protecting DNA from errors and damage: an overview of DNA repair mechanisms in plants compared to mammals. Cell. Mol. Life Sci. **74**: 1693–1709.

Starostina, N.G. and Kipreos, E.T. (2012). Multiple degradation pathways regulate versatile CIP / KIP CDK inhibitors. Trends Cell Biol. **22**: 33–41.

Syed, A. and Tainer, J.A. (2018). The MRE11–RAD50–NBS1 Complex Conducts the Orchestration of Damage Signaling and Outcomes to Stress in DNA Replication and Repair. Annu. Rev. Biochem. **87**: 263–294.

Trolet, A., Baldrich, P., Criqui, M.-C., Dubois, M., Clavel, M., Meyers, B.C., and Genschik, P. (2019). Cell Cycle-dependent Regulation and Function of ARGONAUTE1 in Plants. Plant Cell: tpc.00069.2019.

Verkest, A., Manes, C.-L. de O.C.-L.D.O., Vercruysse, S., Maes, S., Van Der Schueren, E., Beeckman, T., Genschik, P., Kuiper, M., Inze, D., De Veylder, L., Inzé, D., and De Veylder, L. (2005). The Cyclin-Dependent Kinase Inhibitor KRP2 Controls the Onset of the Endoreduplication Cycle during Arabidopsis Leaf Development through Inhibition of Mitotic CDKA;1 Kinase Complexes. Plant Cell **17**: 1723–1736.

De Veylder, L., Beeckman, T., and Inzé, D. (2007). The ins and outs of the plant cell cycle. Nat. Rev. Mol. Cell Biol. **8**: 655–665.

Weimer, A.K. et al. (2016). The plant-specific CDKB1-CYCB1 complex mediates homologous recombination repair in Arabidopsis . EMBO J. **35**: 2068–2086.

Wu, J. et al. (2012). Skp2 E3 Ligase Integrates ATM Activation and Homologous Recombination Repair by Ubiquitinating NBS1. Mol. Cell **46**: 351–361.

Yi, D. et al. (2014). The Arabidopsis SIAMESE-RELATED Cyclin-Dependent Kinase Inhibitors SMR5 and SMR7 Regulate the DNA Damage Checkpoint in Response to Reactive Oxygen Species. Plant Cell **26**: 296–309.

Yoshiyama, K., Conklin, P.A., Huefner, N.D., and Britt, A.B. (2009). Suppressor of gamma response 1 (SOG1) encodes a putative transcription factor governing multiple responses to DNA damage. Proc. Natl. Acad. Sci. **106**: 12843–12848.

Yoshiyama, K.O. (2016). SOG1: A master regulator of the DNA damage responsein plants. Genes Genet. Syst. **90**: 209–216.

Yoshiyama, K.O., Kobayashi, J., Ogita, N., Ueda, M., Kimura, S., Maki, H., and Umeda, M. (2013). ATM-mediated phosphorylation of SOG1 is essential for the DNA damage response in Arabidopsis. EMBO Rep. **14**: 817–822.

Zhao, X.A. et al. (2012). A General G1/S-Phase Cell-Cycle Control Module in the Flowering

Plant Arabidopsis thaliana. PLoS Genet. **8**: e1002847.

Gentric et al., Figure 1

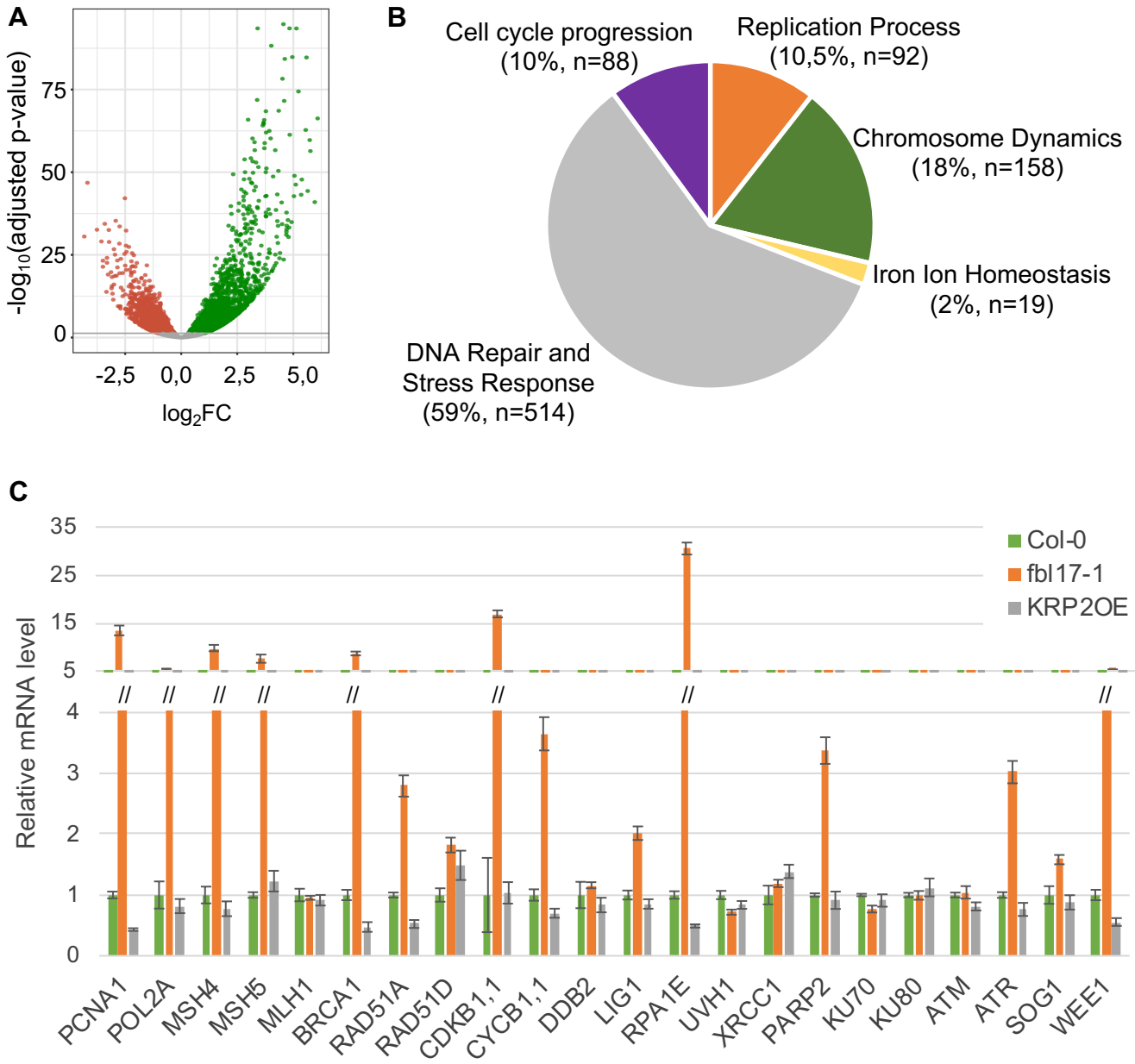

Gentric et al., Figure 2

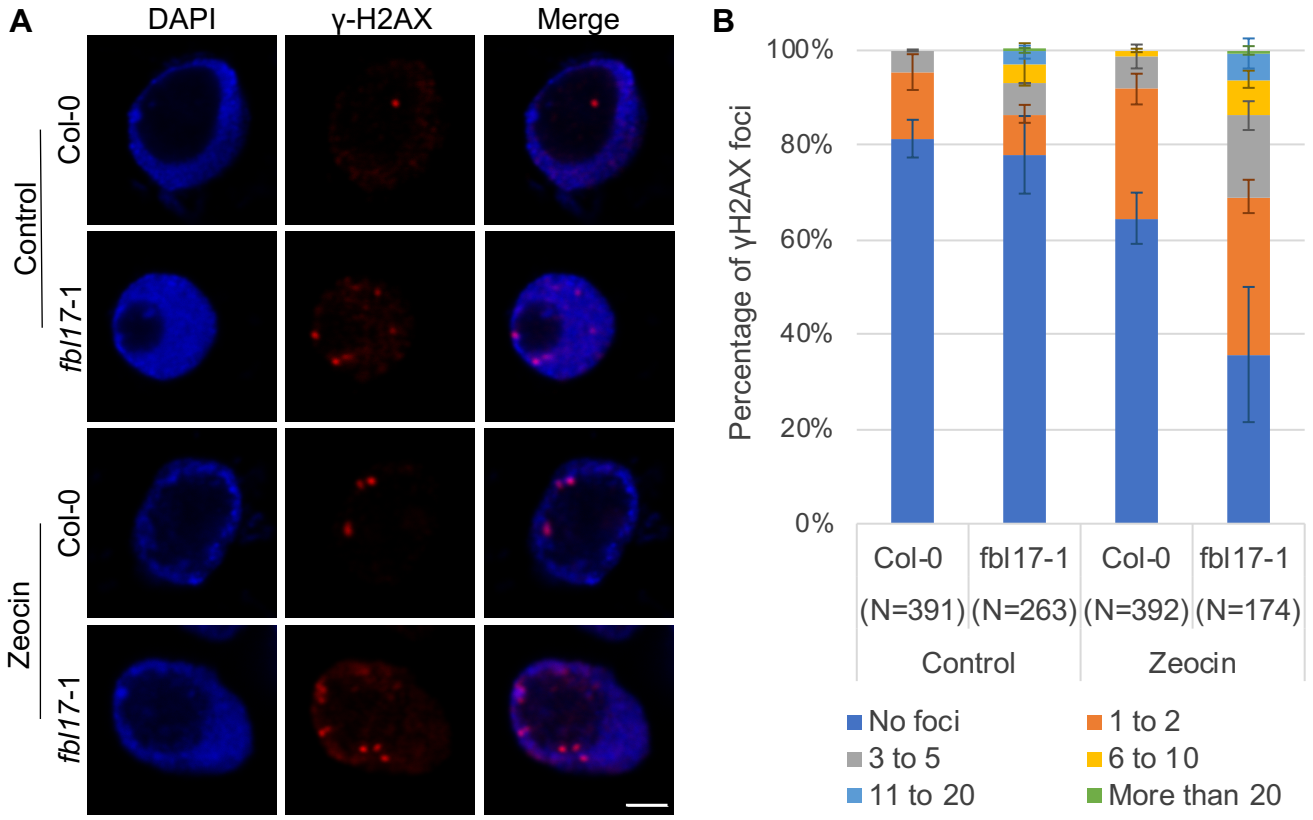

Gentric et al., Figure 3

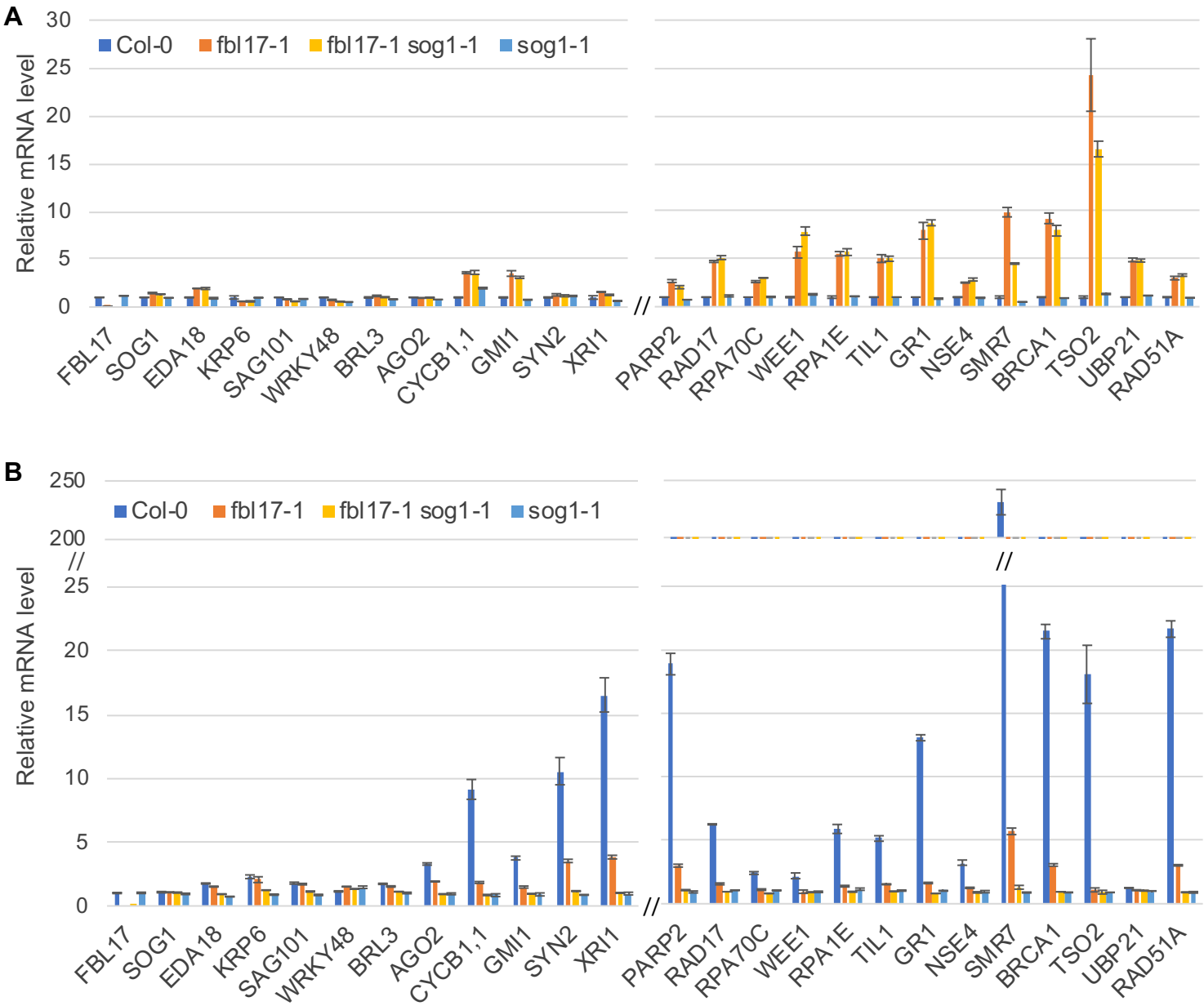

Gentric et al., Figure 4

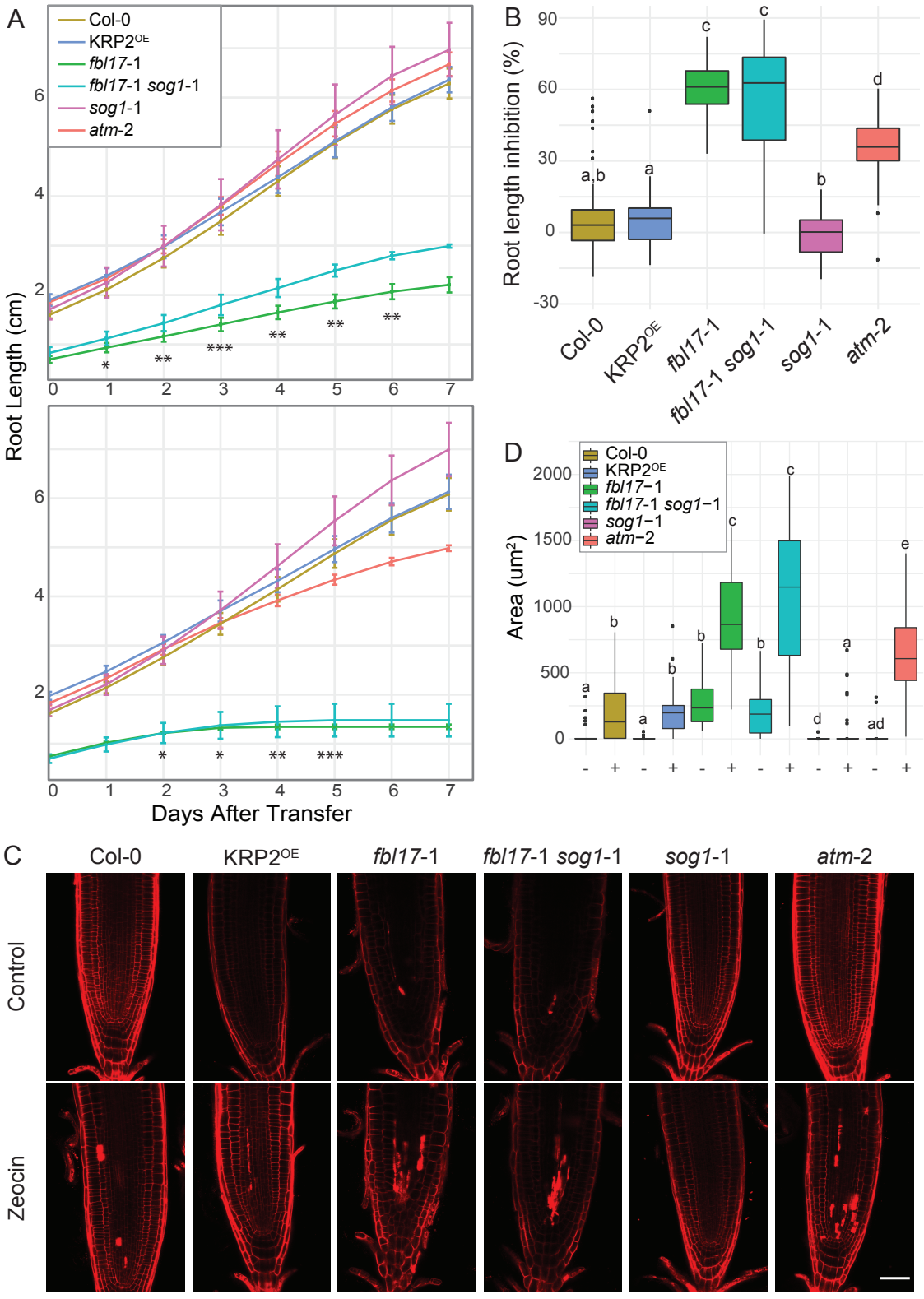

Gentric et al., Figure 5

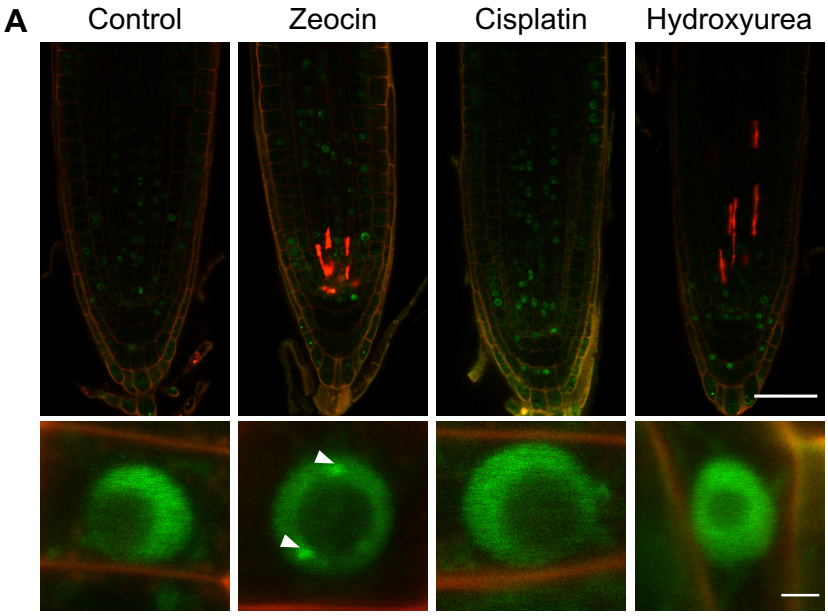

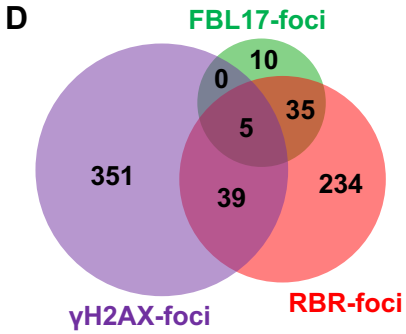

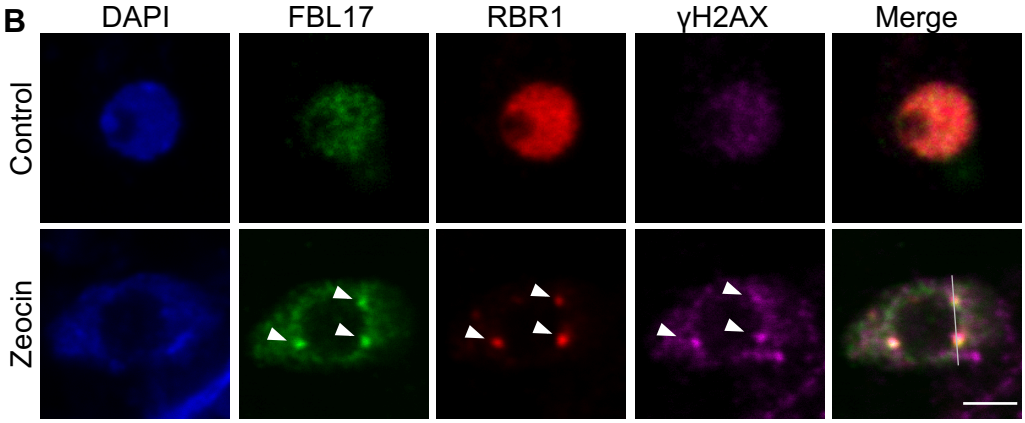

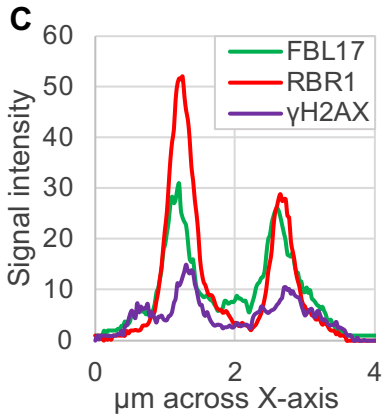

Gentric et al., Supplemental Figure 1

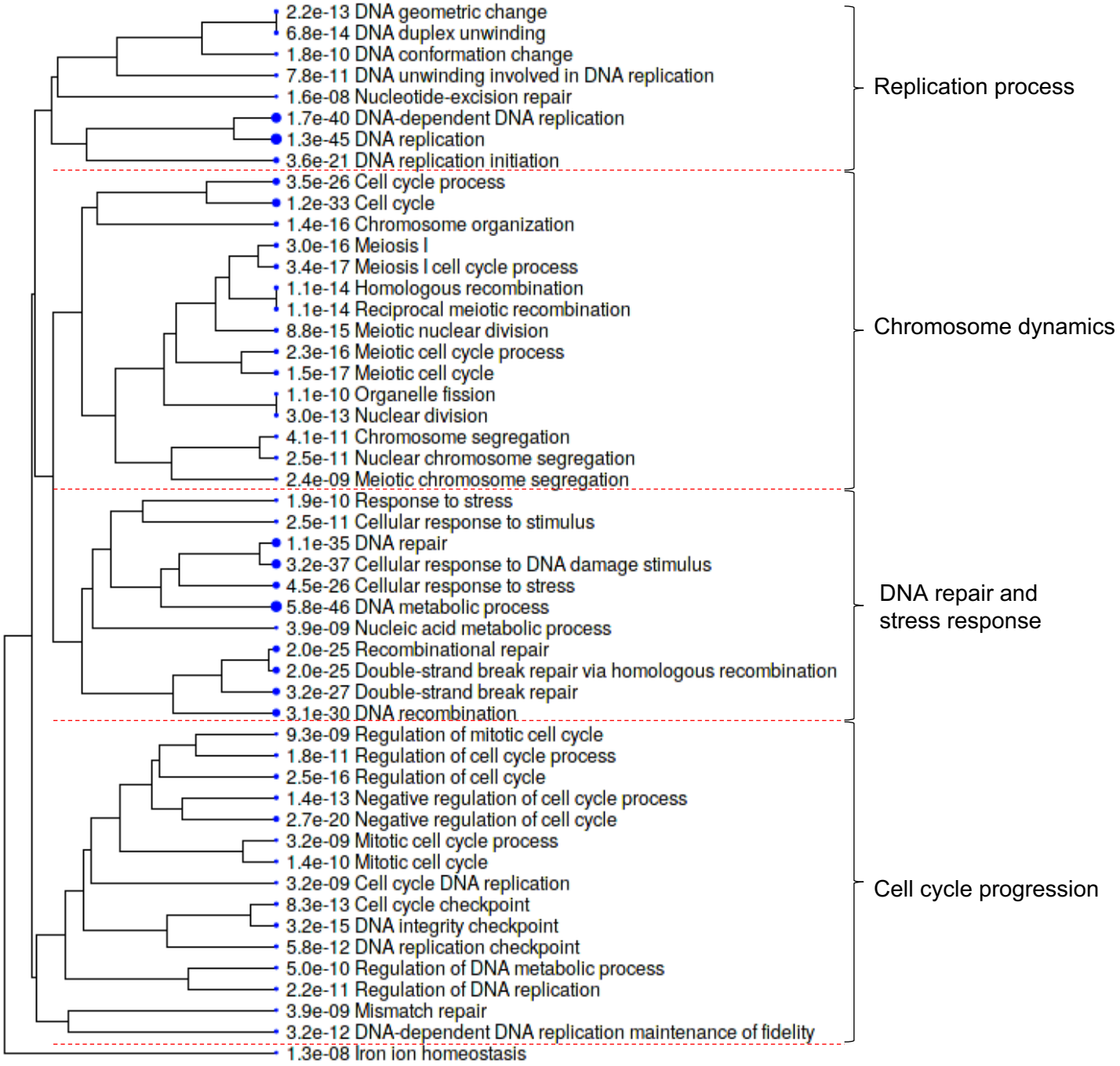

Gentric et al., Supplemental Figure 2

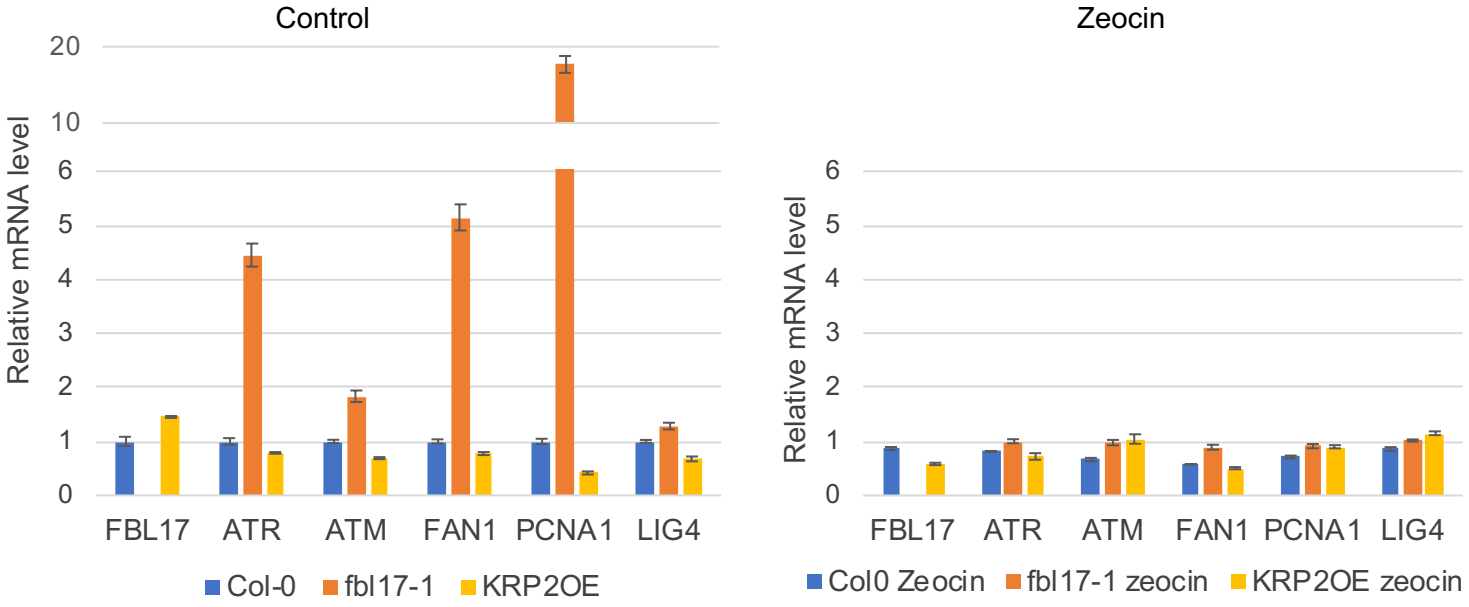

Gentric et al., Supplemental Figure 3

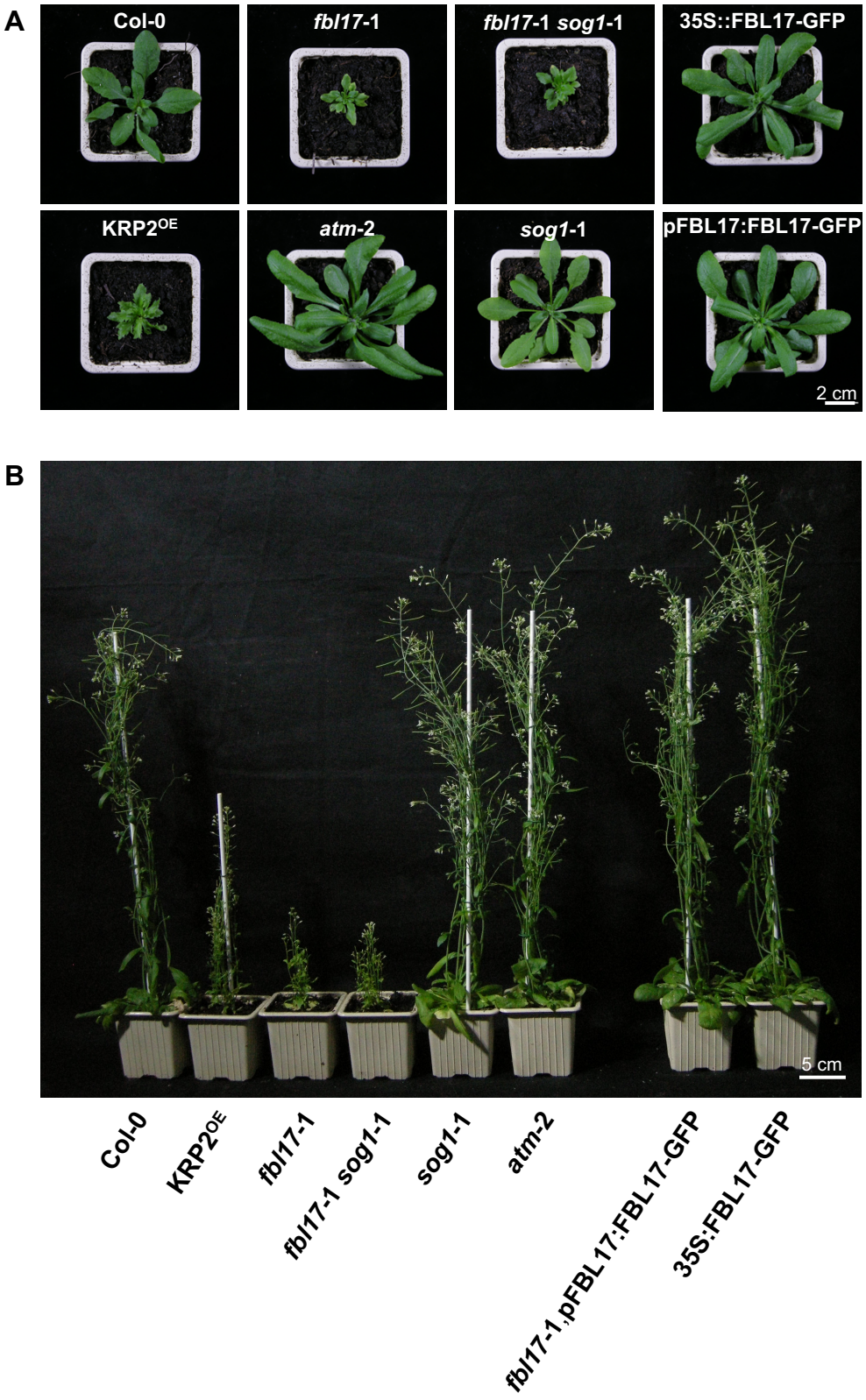

Gentric et al., Supplemental Figure 4